Bacteriophage resistance increases bacterial productivity by shifting population growth dynamics in the soil bacterium *Variovorax* sp.

Authors: Meaghan Castledine[1], Daniel Padfield[1], Rai Lewis[1] & Angus Buckling[1]

[1]College of Life and Environmental Sciences, Environment and Sustainability Institute, University of Exeter, Penryn, Cornwall, TR10 9EZ, U.K.

Corresponding author: Meaghan Castledine (mcastledine96@gmail.com)

Author contributions: MC and AB conceived and designed the study. Experiments conducted by MC. DNA extractions for population sequencing conducted by RL. Bioinformatics conducted by DP and MC. Data analysis conducted by MC. All authors contributed to the writing of the manuscript.

Competing Interests: We have no competing interests

Acknowledgements: We thank Stineke van Houte and Michael Brockhurst for helpful feedback on a manuscript draft. This work was funded by grant no. MR/N0137941/1 for the Great West 4 BIOMED Medical Research Council Doctoral Training Partnership, awarded to the Universities of Bath, Bristol, Cardiff, and Exeter from the Medical Research Council/UK Research and Innovation, awarded to MC. This work was supported by NERC awards NE/V012347/1 and NE/S000771/1 awarded to AB. DP is funded by a NERC independent research fellowship (NE/W008890/1).

Data availability: All data and R codes used in the analysis will be made available on GitHub. Assemblies and sequencing data will be available from ENA.

Abstract

Bacteriophages can be important drivers of bacterial densities, and therefore microbial community composition and function. In response to phage infection, bacteria can evolve resistance while phage can reciprocally evolve to increase infectivity. Coevolutionary arms-races between bacteria and phage have been studied in many model systems and in pairs isolated from natural samples. However, how multiple bacteria-phage pairs coevolve simultaneously within a community is poorly understood. Here, we examine how three pairs of coexisting soil bacteria (*Ochrobactrum* sp., *Pseudomonas* sp., and *Variovorax* sp.) evolve with three species-specific bacteriophages over eight weeks of experimental evolution, both as host-parasite pairs in isolation and as a mixed community. Coevolution was very limited, with two phages going extinct after two weeks and *Ochrobactrum* phage increasing in infectivity without comparable reciprocal increases in bacterial resistance. One surprising finding was that *Variovorax* sp. increased in density following phage extinction, above that of no-phage controls. We examined the mechanisms behind this density increase through common garden experiments, growth curves, supernatant assays, and sequencing. Our results showed that this density increase resulted from genetic changes and was associated with phage resistance. Growth curves demonstrated that phage resistance shifted population growth curves such that density was higher in the death-phase. That resistance to lytic phage can improve host densities has implications for wider ecology and phage therapy where lytic phages are presumed to have negative effects on their hosts.

Introduction

Bacteriophages can be important drivers of bacterial ecology and evolution [1]. Not only do they lyse bacteria, but the emergence of phage resistance also has important implications for host fitness by imposing growth rate costs, virulence trade-offs, and can even reverse antimicrobial resistance [1–4]. As such, phages are hypothesised to prevent overgrowth of bacteria and maintain community diversity [5]. For instance, phages can limit densities of *Vibrio cholerae*, therefore reducing the likelihood of cholera outbreaks [6]. In recent years, there has been growing interest in the use of phages as therapeutics due to rising antibiotic resistance [7, 8]. Therefore, understanding how bacteria and phage interact has implications in ecological and applied contexts.

Phages can continue to replicate following bacterial resistance evolution by either growing on susceptible populations or coevolving to maintain infectivity [9]. Bacteria-phage coevolution has been characterised in several model systems including *Escherichia coli* [10], Pseudomonads (*P. fluorescens* [11], *P. syringae* [12]), and *Staphylococcus aureus* [13] and can have variable dynamics, such as arms-race or fluctuating selection [14]. Environmental conditions can also play a major role [1], including the importance of being embedded in complex communities. While studies have characterised coevolution in natural, environments, (soil [15], plant leaves [16], digestive tracts [17], and marine systems [18]), these studies typically focus on a single bacteria and phage pair, whereas in nature multiple bacteria-phage pairs coexist together.

There are good reasons to expect that coevolutionary dynamics will be affected by the presence of other coevolving species pairs as a result of changes in ecological dynamics and genetic trade-offs [19–24]. A general expectation is that pairwise reciprocal selection will be weakened in more complex communities as a result of lower encounter rates resulting in less pronounced and slower coevolution [25]. To investigate the importance of multiple co-occurring coevolving pairs, we used a three-species bacterial community including *Ochrobactrum* sp., *Pseudomonas* sp., and *Variovorax* sp., each of which has a species-specific lytic bacteriophage [26]. We coevolved these species for eight weeks in the presence and absence of community members, with and without phage.

We only observed limited coevolution (one cycle of resistance and infectivity) for *Ochrobactrum* and its phage, with no coevolution detected between the other pairs. However, we observed an interesting interaction between *Variovorax* and its phage: phage increased *Variovorax* densities in both monoculture and polyculture. Phages have been hypothesised to increase bacterial densities by reducing intraspecific competition through slowing of growth rates or facilitating diversification into separate ecotypes [15, 27]. However, mechanisms have yet to be identified. Here, we report on the population and evolutionary dynamics between *Variovorax* and its phage and conduct experiments to determine the mechanisms responsible for phage-mediated increases in *Variovorax* densities.

Materials and Methods

Experimental evolution

103 Species isolates were originally obtained from soil and identified as: *Ochrobactrum*
104 sp., *Pseudomonas* sp., and *Variovorax* sp. These species have unique colony
105 morphologies when plated onto King's medium agar (KB agar) and can stably coexist
106 for several weeks [19]. In previous work, species-specific bacteriophages
107 (*Ochrobactrum* phage ORM_20, *Pseudomonas* phage CH7FMC, *Variovorax* phage
108 VAC_51) were identified and characterised for each species [26]. Experimental
109 treatments included: monoculture, monoculture with phage (each bacterial species
110 individually with only its species-specific bacteriophage), polyculture (all three bacteria
111 present) and polyculture with phage (all three bacteria with all three phages present).
112 Each treatment was replicated six times. Each species was grown from one colony
113 (clone) in isolation for two days in 6 mL growth media (1/64 Tryptic Soy Broth (TSB);
114 diluted with demineralised H_2O), static, at 28 °C in 25 mL glass microcosms with
115 loosened plastic lids. Species densities were normalised to ~10^5 CFU/μL as described
116 previously [19, 28]. 10 μL of diluted culture (~10^6 CFUs) of each bacterial species were
117 added to fresh vials. To phage-present cultures, ~10^4 PFUs (plaque forming units)
118 were added (MOI 0.01). Serial 100-fold dilutions (60 μL culture into 6 mL growth
119 media) took place every week for a total of eight weeks. Culture samples were
120 cryogenically frozen at −70 °C in glycerol (final concentration: 25%) every transfer.
121 Cultures were plated every 2nd transfer onto KB agar and incubated for two days at 28
122 ºC. Additionally, phage extractions were performed every 2nd transfer: 900 μL of
123 culture was vortexed with 100 μL chloroform. Vials were then centrifuged at 14000
124 rpm (21100 g; Progen GenFuge 24D centrifuge) for five minutes (mins) and the
125 supernatant isolated. Phage densities were calculated via spot assays: phage cultures
126 were diluted and 10 μL of each dilution was spotted onto soft agar overlays of each
127 bacterium, with 100 μL of overnight bacterial culture added to 7 mL soft KB agar. If

128 phages decreased below detectable densities, extracts were amplified in overnight
129 cultures of ancestral strains of each species and re-spotted to confirm extinction.
130
131 **Measuring phage resistance and bacteria – phage coevolution**
132 We estimated phage resistance to ancestral phage for each species from week two
133 cultures. Additionally, for *Variovorax* cultures, we estimated phage resistance in week
134 eight monocultures (phage present and absent). Twelve colonies were picked from
135 each time point, for each bacterium within each treatment. Colonies were inoculated
136 into 150 µL TSB and grown overnight at 28 °C in 96-well plates. Phage resistance was
137 analysed using spot assays as above with ancestral phage.
138
139 As only *Ochrobactrum* and its phage coexisted for eight weeks, we were only able to
140 characterise coevolution for this pair. Twelve bacterial colonies from each treatment
141 replicate from weeks two, four and six were picked and grown as above. Changes in
142 phage resistance and infectivity were tested by spotting phages from different
143 timepoints (ancestral, two, four and six) against bacteria from the same or past/future
144 timepoints. If bacteria and phage are coevolving via arms-race dynamics, we expect
145 bacteria to be more resistant to phage from the past and more susceptible to phage
146 from future timepoints [11, 29]. If dynamics follow a fluctuating-selection dynamic, we
147 expect bacteria to have greater resistance to contemporary phage populations
148 (Gandon *et al*., 2008).
149
150 **Clonal growth rates**
151 Following the results of experimental evolution, we focussed on *Variovorax* and its
152 phage VAC_51. We first wanted to assess whether higher densities conferred to

153 phage-exposed populations was due to higher growth rates within individual clones
154 (common garden experiments). From week two and four cultures (the weeks
155 preceding and following higher densities), twelve colonies were isolated from each
156 replicate from monoculture treatments. Colonies were individually grown in 1/64 TSB
157 and density normalised as before. To fresh 6 mL 1/64 TSB, ~10^6 CFUs of each clone
158 were added to individual vials. Cultures were grown for 1 week, frozen, and plated
159 from frozen onto KB agar as previous.
160
161 **Clonal and population sequencing and bioinformatics**
162 To gain insight into the mechanism of resistance and whether this could be linked to
163 changes in bacterial density and growth rate, isolates were sent for whole genome
164 sequencing (WGS). Three phage resistant and three phage susceptible clones from
165 three independent week two polyculture lines were selected for whole genome
166 sequencing (WGS). Polyculture lines were selected as these were the only treatment
167 which had phage susceptible and resistant clones coexisting (100% resistance was
168 found in monoculture lines). This allowed for direct comparison between different
169 clones that have evolved from the same starting population but only differed in their
170 resistance profile. DNA extractions were done on each isolate by MicrobesNG using
171 in-house protocols (MicrobesNG Sequencing Service Methods, 2021). WGS was
172 performed by MicrobesNG using an Illumina Novaseq 6000 to create 250 base pair
173 (bp) paired-end reads. In-house processing by MicrobesNG trimmed the adapters and
174 removed reads with a quality <15.
175
176 To try and further understand genetic changes that resulted in increased growth rates
177 of phage resistant *Variovorax*, cultures from week 7 monoculture lines of evolution

178 were sent for population sequencing. Overnight cultures (120 µL frozen stock in 1/64
179 TSB grown shaking at 28 ºC. 1.8 mL was spun at 16000 x g for 5 mins (Progen
180 GenFuge 24D centrifuge). The supernatant was removed and another 1.8 mL of fresh
181 sample was added to each tube and centrifuged for a further 5 mins and supernatant
182 removed. The Qiagen DNeasy Ultra Clean DNA Extraction Kit reagents and protocol
183 were used to extract the gDNA from the cultures. The concentration of gDNA in each
184 sample was determined using the QuBit™ dsDNA HS Assay kit regents and protocol.
185 Sequencing was done by the University of Liverpool's Centre for Genomic Research
186 (CGR) using an Illumina Novaseq to create 150bp paired end reads. The CGR
187 trimmed for the presence of Illumina adapter sequences using Cutadapt (v1.2.1) and
188 removed reads with a minimum quality score of 20 and which were shorter 15bp in
189 length.
190
191 For both clonal and population sequencing, we further filtered the trimmed reads to
192 remove Illumina adapter sequences and for reads with a quality score below 10 using
193 TrimGalore (v0.6.4_dev). We used the breseq pipeline (v0.36) – a computational tool
194 for analysing short-read DNA data - to map the trimmed reads to a high quality
195 reference genome of *Variovorax* sp. and predict genetic variants [30]. As our reference
196 genome has two contigs, we added the parameters "-c" and "—contig-reference" so
197 that all the sequences are assumed to have the same average coverage and coverage
198 distribution. In the clonal sequencing, 97.6% of reads mapped to the reference
199 genome (minimum of 95.4%) and giving on average ~876,989 reads per replicate
200 (minimum 444,292), with an average coverage of 62.21 (minimum of 31.84). We only
201 investigated genetic variants that were at a frequency of 1 (we do not expect
202 polymorphisms in any of the predicted genetic variants). For the population

203 sequencing, we ran breseq in polymorphism mode (-p). Variants with <5% frequency
204 in the population samples were removed.
205
206 When mutations unique to resistant clones appeared in a hypothetical protein, we
207 aimed to understand the potential role of this protein by simulating its structure. The
208 amino acid sequence of the protein was run through Phyre2 (Protein
209 Homology/analogY Recognition Engine V 2.0) and the top result was selected for
210 predicted protein structure and function [31].
211
212 **Phage resistance and competition assay**
213 We determined if phage resistance conferred a growth rate benefit to *Variovorax*,
214 thereby leading to higher bacterial densities. Twelve clones per replicate from week
215 two monoculture-lines were isolated and grown in 96-well plates with 150 µL TSB.
216 Phage resistance was determined by streaking isolated colonies against the ancestral
217 phage (streak assay). Week two isolates were chosen as this time-point preceded
218 changes in bacterial density from phage exposure and phage extinction. We elected
219 for phage resistant clones generated during experimental evolution (instead of
220 selecting spontaneous mutants) in the hope that resistance mutations/mechanisms
221 (and therefore phenotypic effects) were consistent with those from the evolution
222 experiments. One phage resistant clone from the phage resistance assays was
223 chosen for each replicate (n = 6), and one clone from each no-phage treatment
224 replicate was isolated as a phage susceptible control (n = 6). Each colony was grown
225 individually in 1/64 TSB individually as described previously. In addition, marked
226 (ancestor-cp; chloramphenicol resistance [32]) and unmarked ancestral *Variovorax*
227 sp. were grown. Cultures were diluted to normalise densities as described previously.

228 The unmarked ancestral strain and each phage resistant and susceptible colony was
229 competed against the marked ancestral strain at equal starting densities (~3 x 10^6
230 CFUs of each competitor inoculated (30 µL diluted culture)). Diluted cultures used in
231 inoculation were frozen and plated on KB agar as above for starting density estimation.
232 Cultures were grown for one week as previous and plated from frozen onto KB and
233 KB-chloramphenicol (25 µg/mL) agar. Relative fitness was calculated from the ratio of
234 the estimated Malthusian parameters, $m_{resistant}$, $m_{susceptible}$ or $m_{ancestor}$:$m_{ancestor\text{-}cp}$, which
235 were calculated as $m = \ln(N_1/N_0)$, where N_1 is the final density and N_0 is the starting
236 density [33].
237
238 **Growth curves**
239 Next, we were interested if phage resistance had shifted the growth curve of
240 *Variovorax* populations thereby leading to higher densities at transfer. 120 µL from
241 each monoculture line from week seven were revived in 6 mL growth medium and
242 grown shaking for two days at 28 ºC. Densities were normalised as previous and 10
243 µL was inoculated into fresh growth medium. Every 24 hrs for one week, cultures were
244 vortexed and optical density (OD_{600}; Multiskan Sky) was measured from a 200 µL
245 sample.
246
247 To characterise the log/exponential growth phase of phage resistant and susceptible
248 cultures, week seven cultures were revived as previous and 20 µL of diluted culture
249 (~10^6 CFUs) were inoculated into 180 µL growth medium. Optical density reads were
250 measured every 45 mins for 24 hrs. This experiment provides higher resolution of
251 growth during exponential phase.
252

253 **Supernatant assay**

254 We hypothesised that higher densities and shifts in growth curve may be caused by
255 production of less-toxic metabolites. This hypothesis was tested using a supernatant
256 assay. Here, week seven cultures were revived and normalised as previous using five
257 replicates of resistant and susceptible populations (one replicate each of susceptible
258 and resistant cultures became contaminated and were not used in the experiment).
259 Two replicates of each week seven culture (two technical replicates for each biological
260 replicate) were established to ensure enough supernatant was available for the
261 reciprocal transplant assay. Cultures were grown for one week. On day five, fresh
262 week seven cultures were revived and grown for two days. Week-old cultures were
263 sterilised by passing medium through a 0.22 μm filter syringe. Replicate supernatants
264 from phage resistant and susceptible populations were pooled into separate
265 supernatant stocks. To separate vials, 3 mL of phage resistant and susceptible
266 supernatant was added to 25 mL vials. Two-day (fresh) culture densities were
267 normalised and each culture was inoculated into both supernatant types. This
268 established two controls in which cultures were grown in the same supernatant (e.g.
269 phage resistant in phage resistant supernatant) and treatments in which cultures were
270 transplanted into the opposite supernatant (e.g. phage resistant in phage susceptible
271 supernatant and vice versa). Cultures were grown for two days and plated as previous.

272

273 **Statistical analyses**

274 All data were analysed using R (v.4.2.1) in RStudio [34] and all plots were made using
275 the package '*ggplot2*' [35]. Model simplification was conducted using likelihood ratio
276 tests and Tukey's post hoc multiple comparison tests were done using the R package
277 '*emmeans*' [36]. Phage resistance was analysed for week two cultures in a linear

278 model with the proportion of phage resistant isolates (arcsine transformed) analysed
279 against interacting effects of treatment (monoculture / polyculture) and species. To
280 assess whether *Ochrobactrum* had coevolved with phage, the proportion of phage
281 susceptible isolates was analysed in a generalised linear model mixed effects model
282 with interacting fixed effects of phage time, bacteria time, and treatment (monoculture
283 or polyculture) with a binomial error structure and a random effect of treatment
284 replicate.
285
286 *Variovorax* densities were analysed in a linear mixed effects model with density (log10
287 CFU/mL) tested against interacting fixed effects of phage exposure, culture type
288 (polyculture or monoculture) and time (weeks two, four, six, eight) with a random effect
289 of treatment replicate. Clonal densities (log10 CFU/mL) from common garden
290 experiments were analysed against interacting fixed effects of phage exposure and
291 time (week two or four) with random effects of treatment replicate and block
292 (experiment conducted in two blocks for feasibility). In competition assays, relative
293 fitness was analysed in a linear model with a fixed effect of competitor (ancestor,
294 phage resistant or susceptible).
295
296 One week growth curves were analysed in a mixed effects model with optical density
297 tested against a fixed term of day and interacting fixed effects of treatment (phage
298 resistant / susceptible) and a quadratic term of day to account for the non-linear
299 relationship. A random effect of treatment replicate was included. 24-hour assays of
300 bacterial growth were used to estimate exponential growth rate. One replicate was
301 removed from the no-phage treatment for failing to grow. Per replicate, exponential
302 growth was estimated using rolling regression, taking the steepest slope of the linear

303 regression between OD_{600} and time in hours in a shifting window of every nine time
304 points (~6.75 hr). A linear model tested growth rate against treatment.
305
306 The supernatant assay was analysed in a linear mixed effects model with density
307 (log10 CFU/mL) analysed against interacting fixed effects of supernatant type and
308 original treatment with a random effect of treatment replicate.
309
310 To test whether consistent genetic differences occur within treatments, we performed
311 nonmetric multidimensional scaling on the Euclidean distance matrix of SNPs/indels
312 and their proportions in each population using '*metaMDS*' in the R package '*vegan*'
313 [37]. Nonmetric multidimensional scaling aims to collapse information from multiple
314 dimensions (i.e., from different populations and multiple SNPs/indels per population)
315 into just a few, allowing differences between samples to be visualized and interpreted.
316 Permutational ANOVA tests were run using '*vegan::adonis*', with Euclidean distance
317 as the response term and treatment as the predictor variable. Additionally, we
318 analysed whether evolution with phage affected the genetic difference of each
319 population (phage, no phage) from the ancestral population. The genetic distance from
320 the ancestral population was calculated as the sum of the difference of the proportion
321 of each SNP/indel in each population from the ancestral proportion. Genetic distance
322 was then analysed in a linear model analysing distance against phage
323 presence/absence.
324
325 **Results**
326 **Phage resistance and bacteria-phage coevolution**

327 Two bacteriophages, for *Pseudomonas* and *Variovorax*, went extinct after just two-
328 four weeks, therefore we estimated phage resistance at week two. Here, phage
329 resistance levels were species specific (ANOVA comparing models with and without
330 species x treatment interaction: $F_{2,29}$ = 3.40, p = 0.047; Figure S1). For *Ochrobactrum*,
331 phage resistance was inhibited in polyculture with no resistant clones while in
332 monoculture 54.2% (SE (standard error) ±20.8) clones evolved resistance (Tukey
333 HSD comparing resistance in polyculture to monoculture: estimate = -0.873, t-ratio =
334 -3.983, p-value <0.001; Figure S1). Similarly, *Pseudomonas* did not evolve resistance
335 in polyculture while 6.94% (SE ±4.52) of clones were resistant in monoculture;
336 although this was not significantly different (Tukey HSD: estimate = -0.157, t-ratio = -
337 0.753, p-value = 0.457; Figure S1). *Variovorax* evolved 100% resistance in
338 monoculture and 90.3% (SE ±6.6) resistance in polyculture which was non-
339 significantly different (Tukey HSD: estimate = -0.215, t-ratio = -1.027, p-value = 0.313;
340 Figure S1).
341
342 As only *Ochrobactrum* coexisted with its phage (Figure S2, S3), we determined if
343 coevolution had occurred by measuring the resistance of bacteria to phage both within
344 and between time points. In polyculture, low frequency resistance (4.17%, SE ± 2.4%)
345 was detected against ancestral phage only at week six, ruling out significant
346 coevolution. In monoculture, 54.2% (SE ± 20.8%) of clones were resistant to the
347 ancestral phage by week two. Phage infectivity increased through time (ANOVA
348 comparing models with and without phage time: χ^2_3 = 122.7, p <0.001; Tukey HSD
349 comparing phage infectivity between ancestral phage, time-points two or four to six: p
350 <0.001; Figure S4). Mean bacterial susceptibility generally increased (resistance
351 declined) at week four (ANOVA comparing models with and without bacterial time-

352 point: χ^2_2 = 27.52, p < 0.001; Tukey HSD comparing resistance between weeks two
353 and four: estimate = -1.12, z-ratio = -4.76, p <0.001; weeks four and six: estimate =
354 0.972, z-ratio = 4.09, p <0.001) then increased at week six back to levels non-
355 significantly different to week two (Tukey HSD weeks two and six: estimate = -0.15, z-
356 ratio = -0.72, p = 0.752). However, bacteria from each time point showed similar
357 patterns of resistance to phages isolated from past, contemporary, and future time-
358 points (ANOVA comparing models with and without phage time x bacteria time
359 interaction: χ^2_6 = 11.36, p = 0.078; Figure S4). These results are suggestive of limited
360 asymmetrical coevolution in monoculture with bacteria evolving resistance to phage
361 (although resistance did not go to fixation), and phage slowly evolving increased
362 infectivity against a subset of bacterial mutants through time.
363
364 **Phage increased *Variovorax* density**
365 We observed an interesting interaction between *Variovorax* and its lytic phage that
366 warranted further investigation. Irrespective of ecological context and time, *Variovorax*
367 densities were significantly higher where phage were present ($\bar{x}$ = $10^{7.79}$ CFU/mL,
368 95%CI = $10^{7.74}$ - $10^{7.85}$) rather than absent ($\bar{x}$ = $10^{7.69}$ CFU/mL, 95%CI = $10^{7.63}$ - $10^{7.74}$;
369 ANOVA comparing models with and without phage: χ^2_1= 7.21, p = 0.007; Tukey HSD:
370 p = 0.013; Figure 1; other species and phages densities presented in Figure S2 and
371 S3). While in weeks two and four, *Variovorax* densities were higher in polyculture
372 compared to monoculture, this difference became non-significant at weeks six and
373 eight (interaction between time and treatment: χ^2_3= 31.54, p < 0.001; Table S1). Phage
374 densities did not differ between monoculture ($\bar{x}$ = $10^{4.50}$ CFU/mL, SE = 0.20) or
375 polyculture ($\bar{x}$ = $10^{4.25}$ CFU/mL, SE = 0.13), and phages in all replicates went extinct
376 after week two (Figure S3).

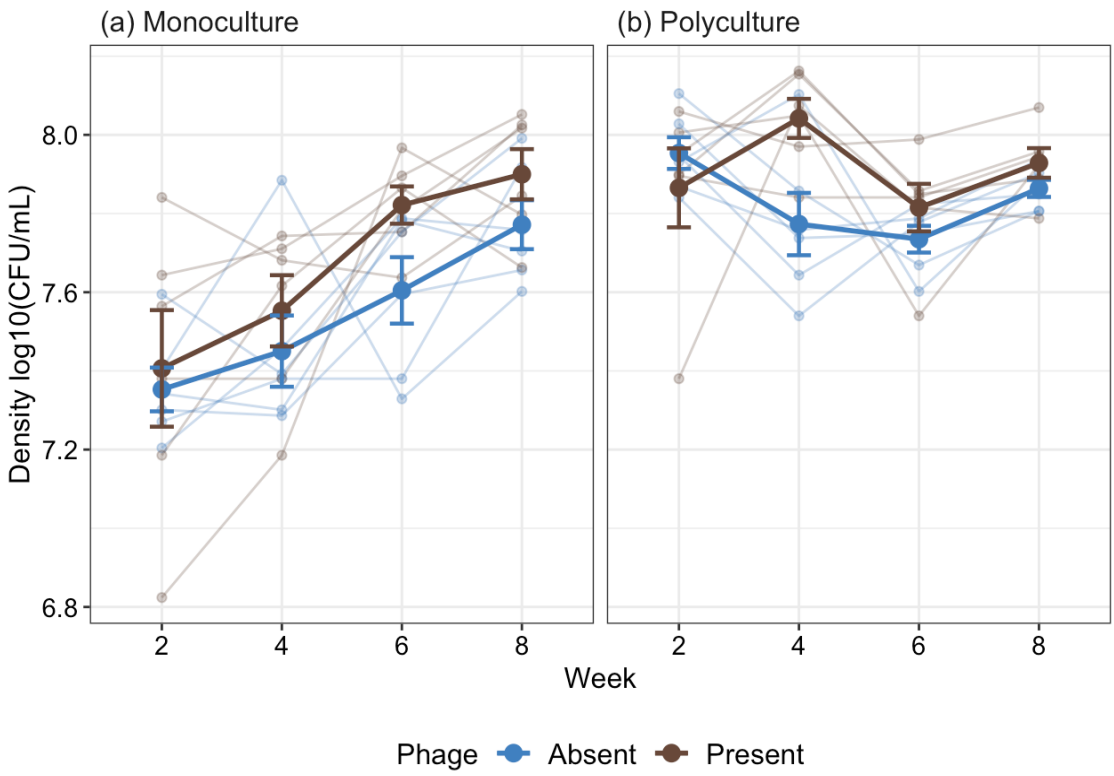

Figure 1. Changes in *Variovorax* density over eight weeks in (a) monoculture and (b) polyculture (two other bacterial species present) in the absence (blue) and presence (brown) of bacteriophage. Large points with bars and lines represent the means with standard errors. Small points and lines represent separate treatment replicates.

Phage resistant clones have higher densities than phage susceptible clones

To assess whether higher densities in phage-exposed populations was likely a result of a genetic change (as opposed to epigenetic or physiological), we measured the densities of individual clones (isolated from weeks two (pre phage loss) and four (post phage loss) from monoculture treatments) grown in isolation in common garden experiments. All clones isolated from phage treatments were phage resistant as phage resistance reached fixation in monoculture, while all clones from the no-phage treatment were susceptible. Consistent with the population dynamics during

experimental evolution, clones isolated from phage-exposed replicates had significantly higher densities ($\bar{x}$ = $10^{7.51}$ CFU/mL, 95%CI = $10^{5.60}$ - $10^{9.41}$) than phage-unexposed clones ($\bar{x}$ = $10^{7.29}$ CFU/mL, 95%CI = $10^{5.38}$ - $10^{9.19}$; ANOVA comparing models with and without phage: χ_1^2= 6.60, p = 0.102; Tukey HSD: p = 0.018; Figure 2). Additionally, there was a significant independent effect of time with clones from week four ($\bar{x}$ = $10^{7.49}$ CFU/mL, 95%CI = $10^{5.30}$ - $10^{9.68}$) reaching higher densities than clones from week two ($\bar{x}$ = $10^{7.31}$ CFU/mL, 95%CI = $10^{5.12}$ - $10^{9.49}$; Tukey HSD: p < 0.001; Figure 2). Overall, these results suggest effects imposed by phage were hereditary as phage did not need to be actively present for effects to be observed.

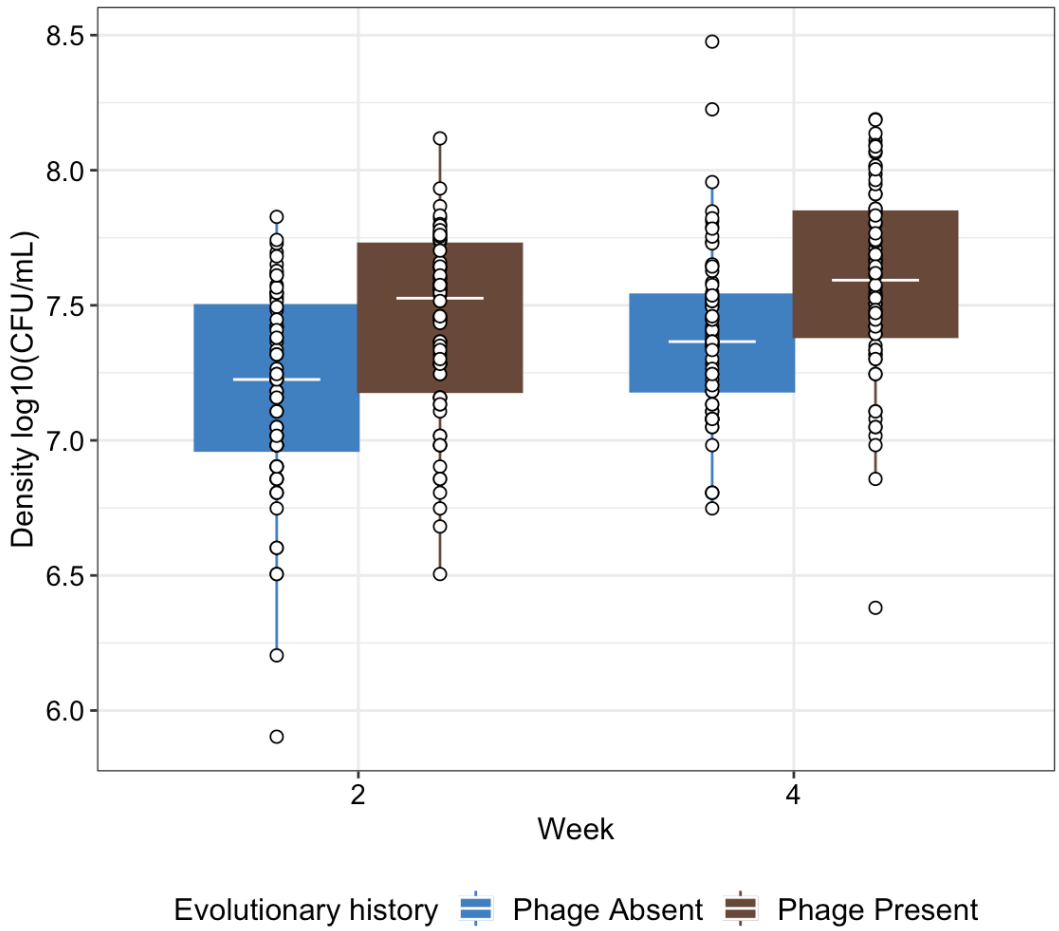

Figure 2. Common garden experiments showing the density of individual clones (points) which have been isolated from evolution lines where phage have been absent or present. Tops and bottoms of the bars represent the 75th and 25th

405 percentiles of the data, the middle lines are the medians, and the whiskers extend
406 from their respective hinge to the smallest or largest value no further than 1.5*
407 interquartile range. Points represent individual clones.
408
409 **Fitness advantage is associated with resistance mutations**
410 Given the consistent higher growth rate that phage exposed populations and phage
411 resistant clones had over phage absent populations and phage susceptible clones,
412 we looked at whether there were underlying genetic changes that could explain this.
413 We sequenced 3 resistant and 3 sensitive clones coexisting within 3 polyculture
414 treatment replicates. Of the phage resistant clones, 2/3 clones had a missense
415 mutation at the same locus (gene ID: 01575) and 1 had a substitute mutation at a
416 nearby locus (gene ID: 01584; 10.4k base pairs downstream; this was also the only
417 mutation in this clone) that was not found in phage susceptible isolates. No other
418 mutations were found at the same loci across clones. While identified in a hypothetical
419 protein, the predicted protein based on amino acid sequence of 01575 suggests that
420 the mutation occurred in a gene responsible for a membrane protein with 99%
421 similarity to cellulose synthase (Figure S5). Single point mutations and receptor loss
422 are consistent with surface modification forms of resistance and suggest the phage
423 has not lysogenised into the chromosome to confer resistance. The phage's DNA
424 sequence has previously shown no genes relating to lysogeny [26]. Generally, few
425 mutations were found, with one resistant clone having four mutations while the other
426 two had only one mutation each. Similarly, one phage susceptible clone had two
427 mutations while the other two had one mutation. 01584 sequence had no comparable
428 genes or protein structures in BLAST or Phyre2.
429

430 We sequenced whole populations taken from seven weeks of evolution in monoculture
431 (*Pseudomonas* and *Ochrobactrum* absent), with the aim of identifying further genetic
432 changes linked to phage resistance and increased density. In total, 239 genetic
433 variants were found in both resistant and susceptible populations. 117 variants were
434 only found in phage resistant populations and 114 were only found in phage
435 susceptible populations. Most variants were found at low frequency (96.8% of variants
436 at <50% frequency) with an average resistant and susceptible population having 147
437 variants. 60 genes had variants only in phage resistant populations, while no variants
438 were found in the same genes in phage susceptible populations; likewise, 64 genes
439 had variants only in phage susceptible populations. 5/6 phage resistant populations
440 had at least one unique genetic variant at high frequency (>50%) while only 2/6 phage
441 susceptible populations had variants at a high frequency, suggesting specific
442 mutations were selected by phage. 2/6 different phage susceptible populations
443 (distinct to the other susceptible populations mentioned in the previous sentence) had
444 unique variants in *cysB* gene at >50% frequency, however 11/12 populations had
445 variants in this gene unrelated to treatment differences. While we did not observe
446 mutations in 01575 (mutation found in 2/3 clones above), mutations were found in
447 01584 (mutation found in 1/3 clones above) in 4/6 phage resistant populations (92.7%,
448 68.2%, 12.3%, 9.6%). Mutations selected to high frequency were also found in *prpR*
449 (69.3% in 1 population; transcription regulator gene) and in five other hypothetical
450 proteins or intergenic regions (Figure 3). The lack of convergence suggests phage
451 resistance may be maintained by several different mechanisms that have the same
452 phenotypic effects (resistance and higher population density). As a result, we did not
453 find phage presence significantly differed in genetic composition (PERMANOVA: $F_{1,10}$
454 = 0.889, p = 0.81, Figure S6) or distance from the ancestral genome (ANOVA: $F_{1,10}$ =

455 0.547, p = 0.477). Overall, evidence from fixation of resistance (100% clones tested
456 being resistant to phage), unique mutations and common garden experiments suggest
457 a link between resistance and phenotypic increases in population density; however,
458 mechanistic links cannot be made between genotypes and phenotypes owing to the
459 lack of convergent evolution.

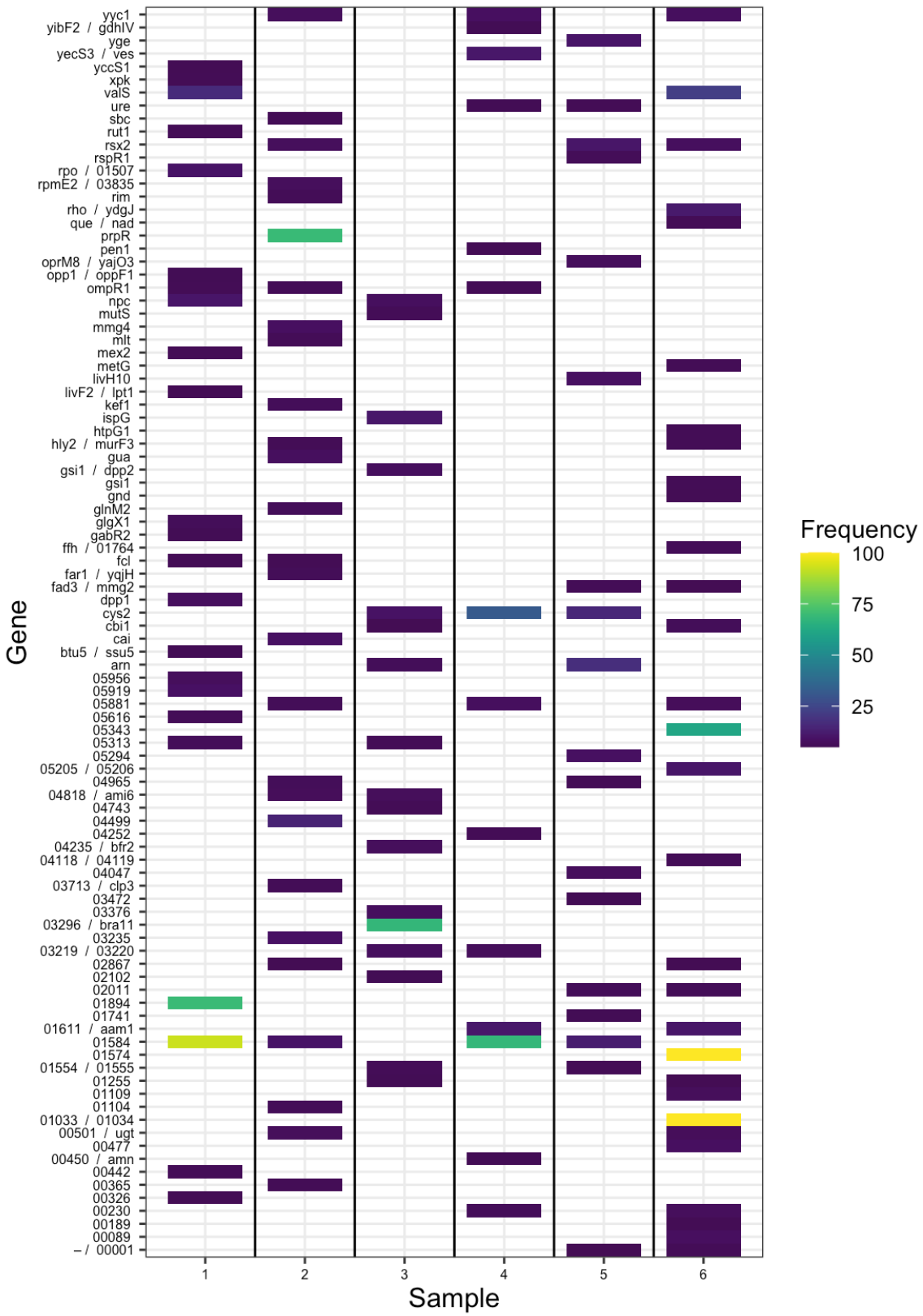

460

461 **Figure 3. The frequency of genetic variants found in phage resistant but not**

462 **phage susceptible populations.** Where multiple variants are found in the same

463 gene, the average has been presented for space purposes. Each replicate population

464 is identified on the x-axis. Genes of known function are named on the y-axis while
465 hypothetical proteins are given a numerical denomination. Gene names separated by
466 a forward slash indicate mutations in intergenic regions. Samples indicate each of the
467 six replicate populations that evolved in the presence of phage.
468
469 **Phage resistant clones do not have a fitness advantage**
470 We next determined whether phage resistance conferred a fitness advantage in the
471 absence of phage. In competition assays with a marked ancestral strain, relative
472 fitness was not significantly affected by phage resistance ($F_{2,15} = 0.460$, $p = 0.640$;
473 Figure 4). The greater density associated with resistance did not therefore result in a
474 competitive fitness advantage.
475

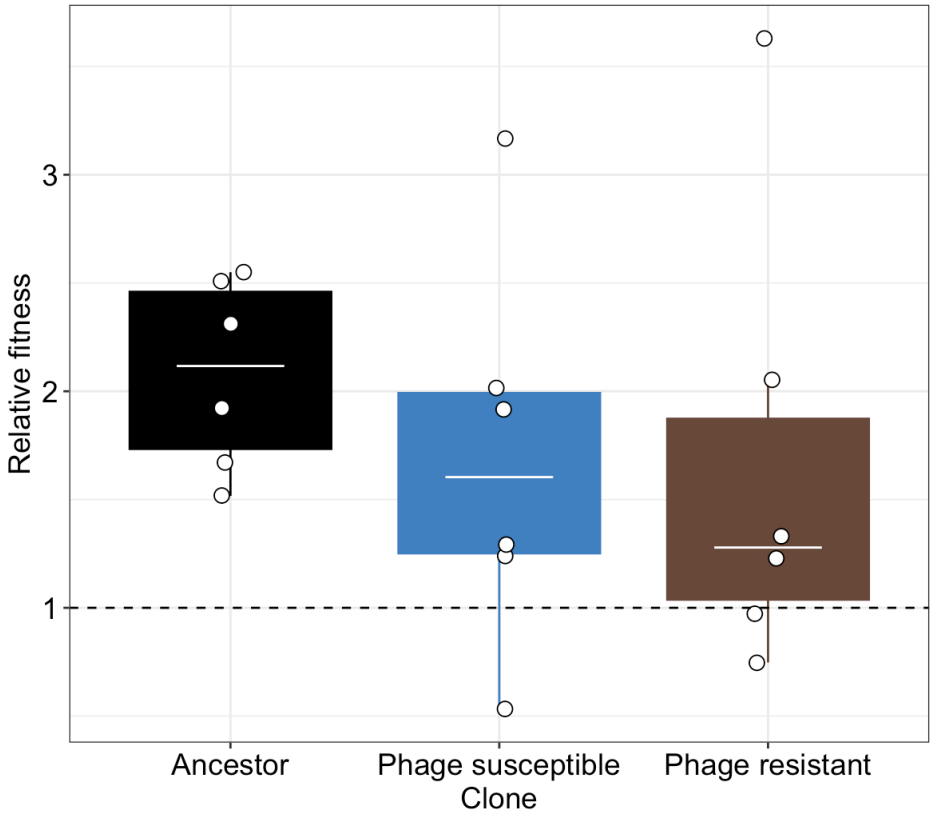

476

Figure 4. Relative fitness of ancestral, phage susceptible and resistant isolates against a marked ancestral strain of *Variovorax*. Points represent independent replicates. Tops and bottoms of the bars represent the 75th and 25th percentiles of the data, the middle lines are the medians, and the whiskers extend from their respective hinge to the smallest or largest value no further than 1.5* interquartile range.

Phage resistance affects growth dynamics

We next investigated if density benefits resulting from resistance arose from changes in growth dynamics. This may have arisen if, for example, logistic growth rates of resistant isolates were slowed, resulting in resources becoming less exhausted when cultures were transferred to fresh media on day seven. As such, we measured the growth curves of *Variovorax* populations isolated from week seven of experimental evolution over one week. Here, there was a significant interaction between treatment and day of measurement (ANOVA comparing models with and without the interaction: χ_1^2 = 7.25, p = 0.007), suggesting phage resistance had altered population growth dynamics (Figure 5). Consistent with our previous observation based on CFU counts (Figure 2), optical density after one week was higher in phage resistant ($\bar{x}$ = 0.067, 95%CI = 0.062 - 0.072) than susceptible ($\bar{x}$ = 0.057, 95%CI = 0.053 - 0.062) populations (Figure 5). Consistent with an absence of fitness differences between susceptible and resistant isolates (Figure 4), there was no significant difference in exponential growth rate measured in the 24 hr growth rate assay ($F_{1,9}$ = 0.622, p = 0.451) or carrying capacity in the one week growth rate assay (phage resistant: $\bar{x}$ = 0.08, 95%CI = 0.075 – 0.085; phage susceptible: $\bar{x}$ = 0.076, 95%CI = 0.072 – 0.081;

Figure 5). Phage resistant isolates show similar growth dynamics to susceptible isolates, except they show a slower decline in density by day 7.

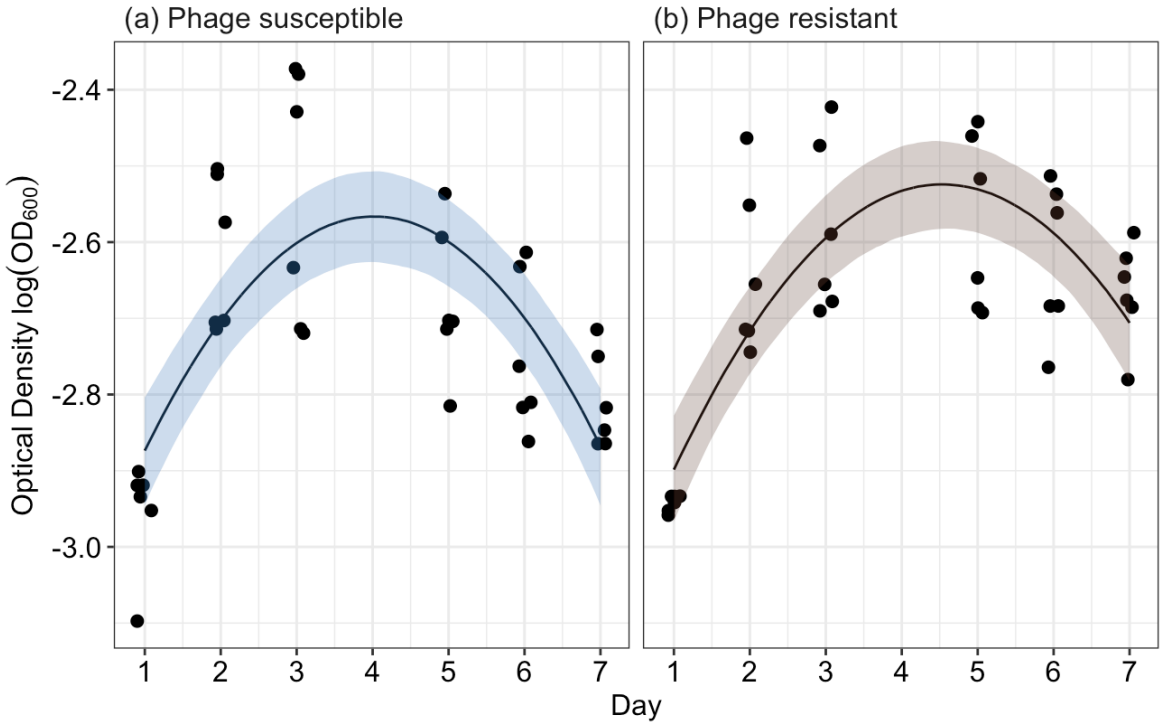

Figure 5. The seven-day growth curves of (a) phage susceptible and (b) phage resistant *Variovorax* populations that had evolved for seven weeks. Points represent individual replicate populations measured repeatedly through time. Solid lines represent the mean predictions and shaded bands represent the 95% confidence intervals.

The supernatant of phage resistant populations is not less toxic

If bacterial populations can maintain a higher density during the stationary/death phase, this suggests that bacteria are potentially producing fewer toxic metabolites and/or are less susceptible to them. We investigated these possibilities by growing week seven populations in spent supernatants from either their own treatment or the opposite treatment. However, population density was non-significantly different between populations irrespective of prior phage exposure (χ_1^2 = 1.48, p = 0.224) or

517 supernatant type (χ_1^2 = 2.12, p = 0.145; interaction between effects: χ_1^2 = 0.148, p =
518 0.7004; Figure 6).

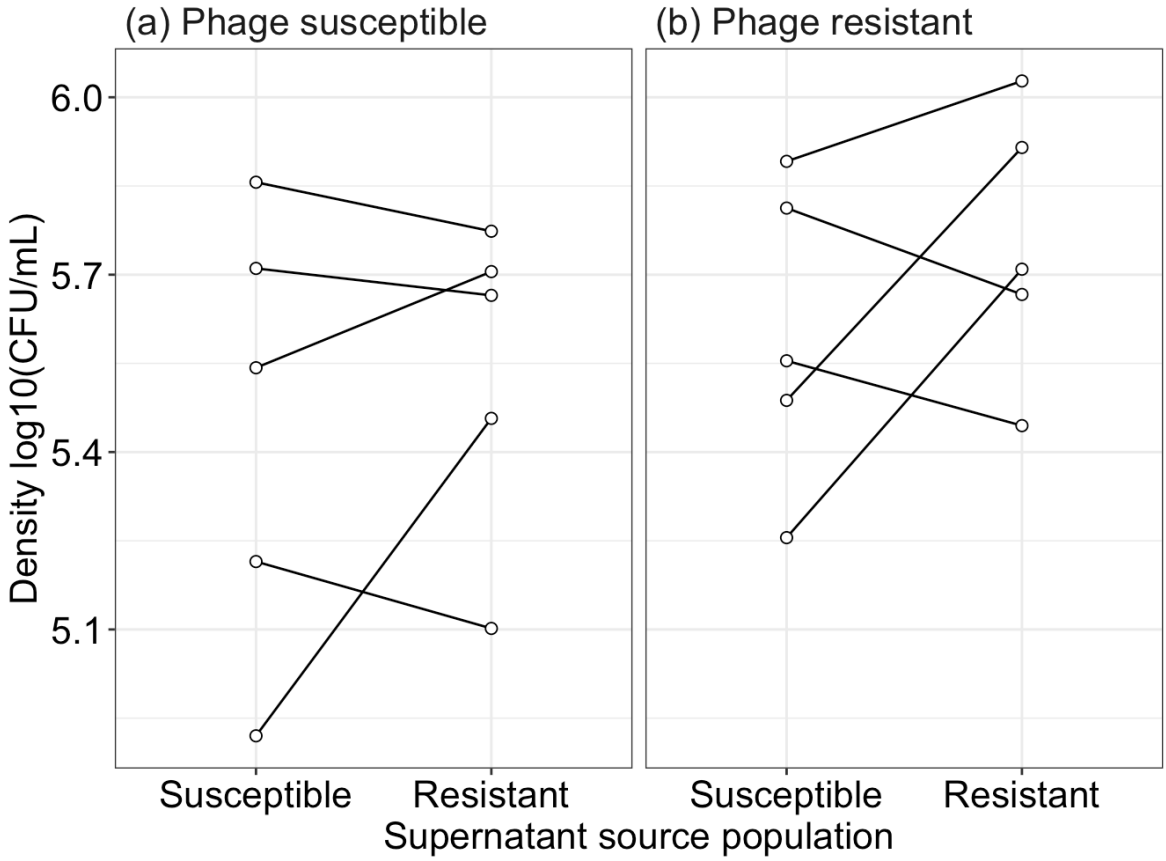

519

520 **Figure 6. Density changes when populations which are (a) phage susceptible**
521 **and (b) phage resistant, are grown in supernatant isolated from either**
522 **population.** E.g. phage susceptible growing in supernatant from phage susceptible
523 populations (same evolutionary history) or phage susceptible growing in supernatant
524 from phage resistant populations (different evolutionary history). Points represent
525 densities of individual replicates while lines indicate the change when that same
526 population is grown in a different supernatant.

527

528 **Discussion**

529 Bacteriophages have been previously shown to positively influence bacterial densities,
530 but only when propagated in monoculture and the mechanism was not determined

531 [15]. Here, we showed that evolved resistance to phage changed the growth curves
532 of *Variovorax* populations resulting in higher densities under the weekly transfer
533 regime. High levels of resistance, and the associated positive effect on density, was
534 observed for several weeks past phage extinction within monocultures (no other
535 bacterial species present) and in a community context. That this effect was consistent
536 in both the presence and absence of other species is particularly interesting as the
537 growth of this species is enhanced by the presence of the other two species [19, 28].
538 As such, irrespective of the metabolic state the bacteria are in (feeding on the media
539 or on supernatant), the phage had a positive effect on *Variovorax* density. Previous
540 work showing a phage-mediated increase in bacterial density occurred in monoculture
541 and not polyculture [15], suggesting a different mechanism to that observed here.
542
543 Phage resistance did not have a significant effect on exponential growth rate but did
544 appear to affect the death phase, with phage resistant populations maintaining a
545 higher density. Although we did not find evidence that this was linked to a change in
546 metabolites produced after one week, it may reflect a broader ability of the bacteria
547 being able to cope in stressful conditions. *Variovorax* is a metabolically plastic species
548 and is capable of being lithoautotrophic or chemoorganotrophic, including the
549 metabolism of toxic or complex compounds [38]. Benefits from phage-exposure were
550 not linked directly to a single phage resistance mutation, however resistance was
551 found to likely emerge via mutations in a surface protein, possibly linked to nutrient
552 acquisition or metabolism, often with missense mutations resulting in a loss of function.
553 Loss of this receptor could have shifted *Variovorax* metabolism to give the effects
554 shown. However, confirming this is challenging due to the complexity of this nutrient
555 medium. Additionally, population sequencing revealed multiple mutations emerging

556 and several reached high frequencies (>50%) in 5/6 phage treatment populations,
557 although with a lack of convergent evolution. All high frequency genetic variants were
558 in hypothetical proteins, making mechanistic inferences impossible within this project.
559 Interestingly, only two no-phage culture had a unique mutation that reached high
560 frequency (>50%) compared to 5/6 phage cultures, suggesting phage presence
561 increased the likelihood of variants reaching a high frequency.
562
563 While resistance was clearly beneficial in the presence and absence of phage,
564 reaching and being maintained at very high frequencies, we did not find any phage
565 resistance emerge in phage-free controls across eight weeks. This was because there
566 was no selective cost or benefit of phage resistant mutants competing against phage
567 sensitive clones in the absence of phage, and hence resistant mutations would not
568 have increased in frequency. Nevertheless, we may expect this resistance-linked
569 growth phenotype to be favoured in highly structured metapopulations, where limited
570 dispersal can result in different patches seeded by single clones with the most
571 productive patches (i.e. those seeded with resistant clones) producing more individual
572 to colonise new patches [39]. The resistance mutations may also allow populations to
573 subsequently explore alternative evolutionary trajectories in the longer term [40].
574
575 In many well-studied model systems bacteria and phage coexist either through
576 resistant and susceptible genotypes being maintained in bacterial populations or
577 phage coevolve to maintain infectivity [9], although there are clear exceptions (e.g.
578 [41]). Here, we found an absence of coevolution in two bacteria-phage pairs with two
579 phages going extinct after two weeks and limited coevolution in one pair. For
580 *Variovorax*, our genetic analyses suggest the receptor for infection was lost which

581 would have made this very challenging for phage to coevolve. Another bacteria and
582 phage used in this study, *Pseudomonas* and phage CHF7MC failed to coexist with
583 phage similarly going extinct after two weeks. *Pseudomonas* phage was driven extinct
584 with little resistance evolution, suggesting the phage was poorly adapted to this host.
585 *Ochrobactrum* and its phage were the only pair to coexist, however phage increased
586 in infectivity asymmetrically to increases in resistance. Studying bacteria-phage pairs
587 beyond model systems, which are presumably often selected precisely because they
588 do clearly coevolve, will provide much greater insight into interactions in bacteria-
589 phage interactions in nature.
590
591 That phage can have effects on hosts following extinction has implications in natural
592 and applied contexts. Phages are sometimes assumed to maintain diversity by
593 regulating host densities through lysis of fast growing populations and imposing fitness
594 costs [5]. Our results suggest lytic phages can sometimes increase bacterial densities,
595 which may contribute to patterns observed in some systems where bacteria such as
596 SAR11 can maintain high densities despite high viral loads [42]. If phages can
597 increase bacterial densities, this may reduce overall diversity by favouring populations
598 with specific phage pairs. If phages can improve the density of soil bacteria, this may
599 have positive impacts on carbon cycling and crop yield. *Variovorax* species, for
600 instance, are symbionts to plants and are found in the rhizosphere where they can
601 improve plant growth [38]. Alternatively, if phages are used therapeutically [7, 8] then
602 density enhancement of target bacterial pathogens is clearly detrimental. Using
603 phages with clinical samples *in vitro* and analysing changes in bacterial genotypes
604 and phenotypes would allow physicians to assess whether a phage is suitable for a
605 patient's treatment [43].

The influence of phages on bacterial populations are highly diverse, making predictions and generalisations challenging from model systems to phages in nature. Our work highlights the surprising outcomes that can arise from bacteria-phage interactions, and that the simple assumption that lytic phages negatively affect host densities or coevolve may not always be true. Wider research analysing the effects of different phages on host bacteria, both during and after phage extinction would give important insight into how phage therapy may affect pathogens during infection and how phages operate in nature.

617 **Supplementary Information**

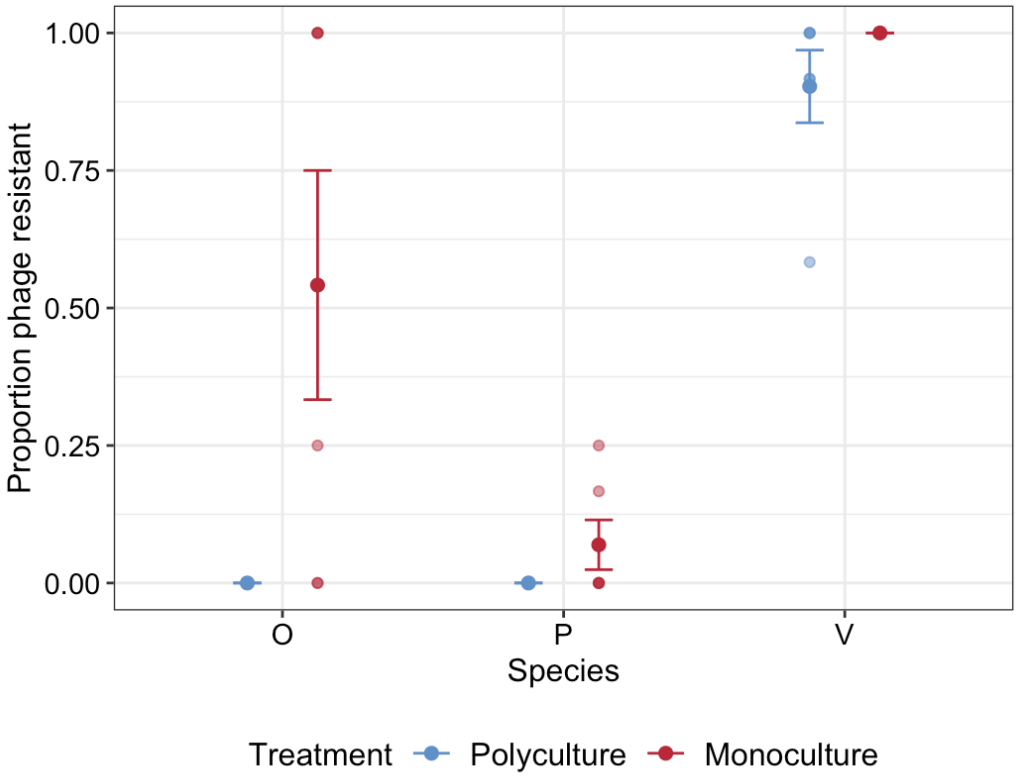

618
619 Figure S1. The proportion of phage resistant bacteria after two weeks evolving with
620 phage in polyculture and monoculture. Points with bars represent the means with
621 standard errors. Individual points represent separate treatment replicates. O,
622 *Ochrobactrum*; P, *Pseudomonas*; V, *Variovorax*.

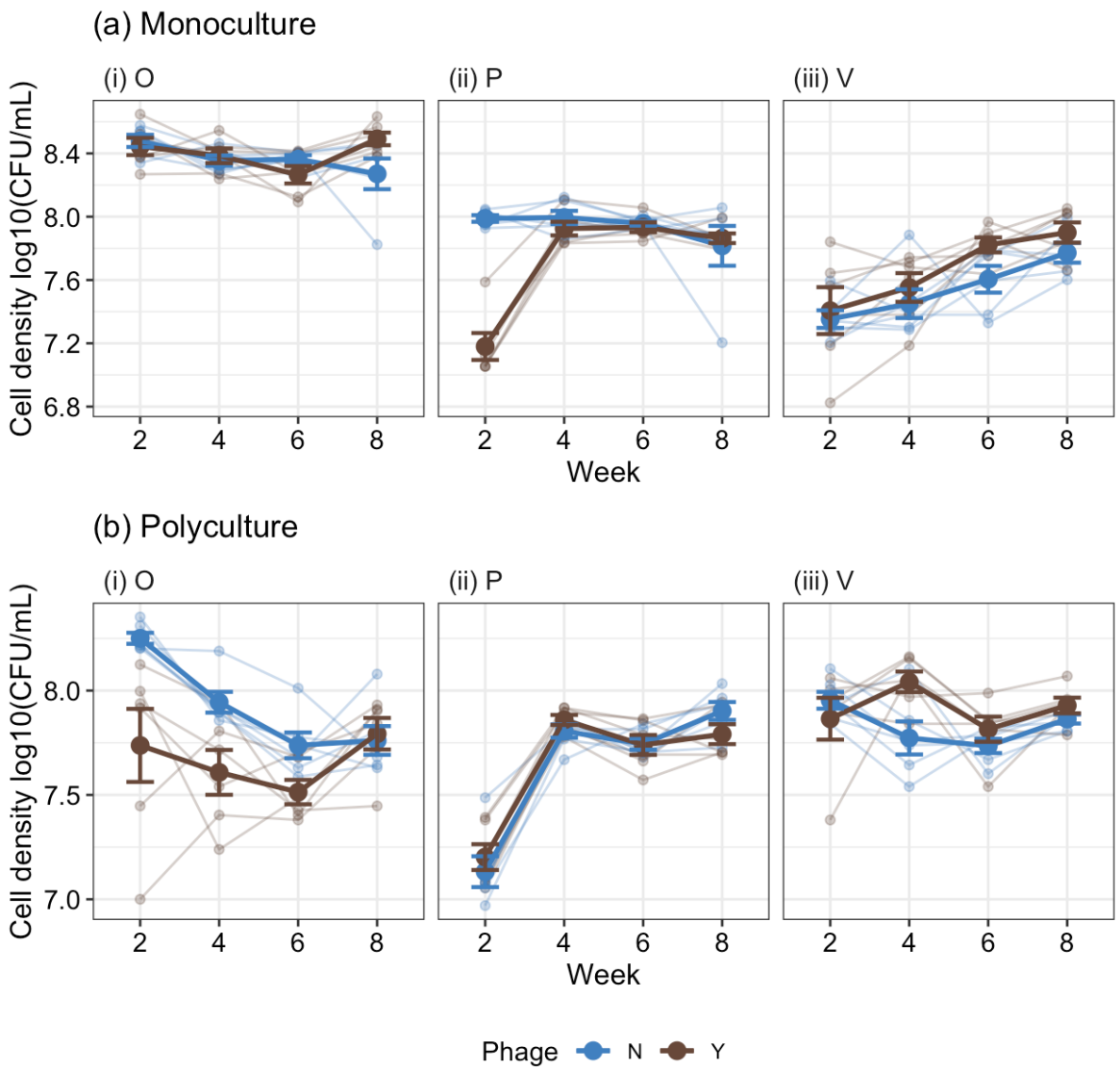

Figure S2. Changes in bacterial density through time in the presence (Y) and absence (N) of phage in (a) monoculture and (b) polyculture. Points with bars represent the means with standard errors. Individual points represent separate treatment replicates. Lines connect points from the same treatment replicate.

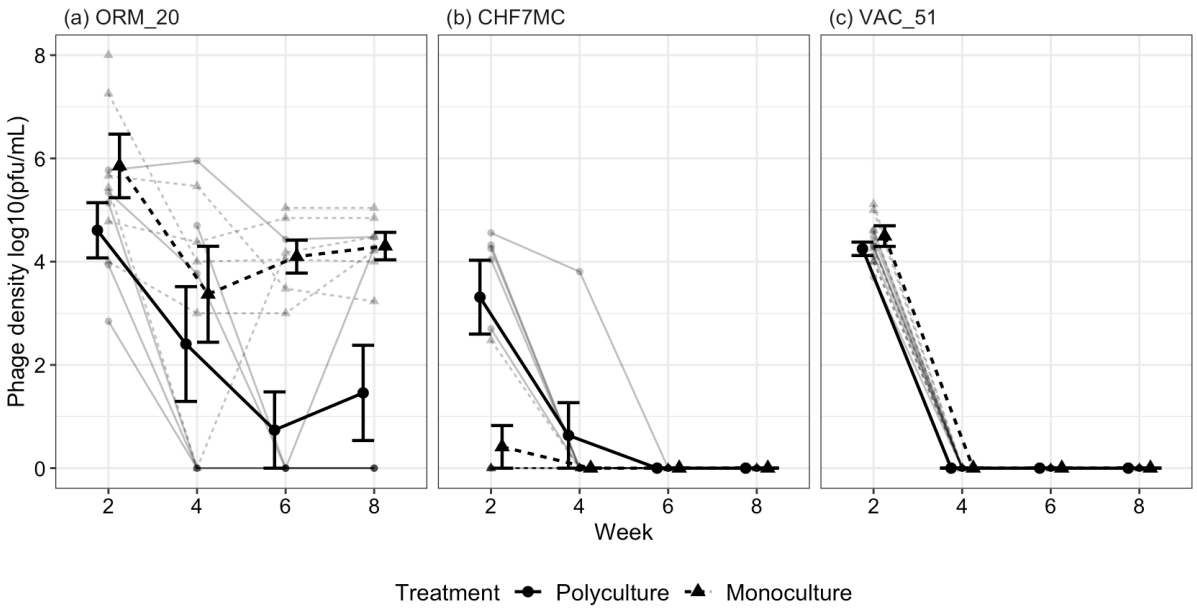

Figure S3. Changes in phage density through time for (a) *Ochrobactrum* phage ORM_20, (b) *Pseudomonas* phage CHF7MC and (c) *Variovorax* phage VAC_51. Points with bars represent the means with standard errors. Individual points represent separate treatment replicates. Lines connect points from the same treatment replicate.

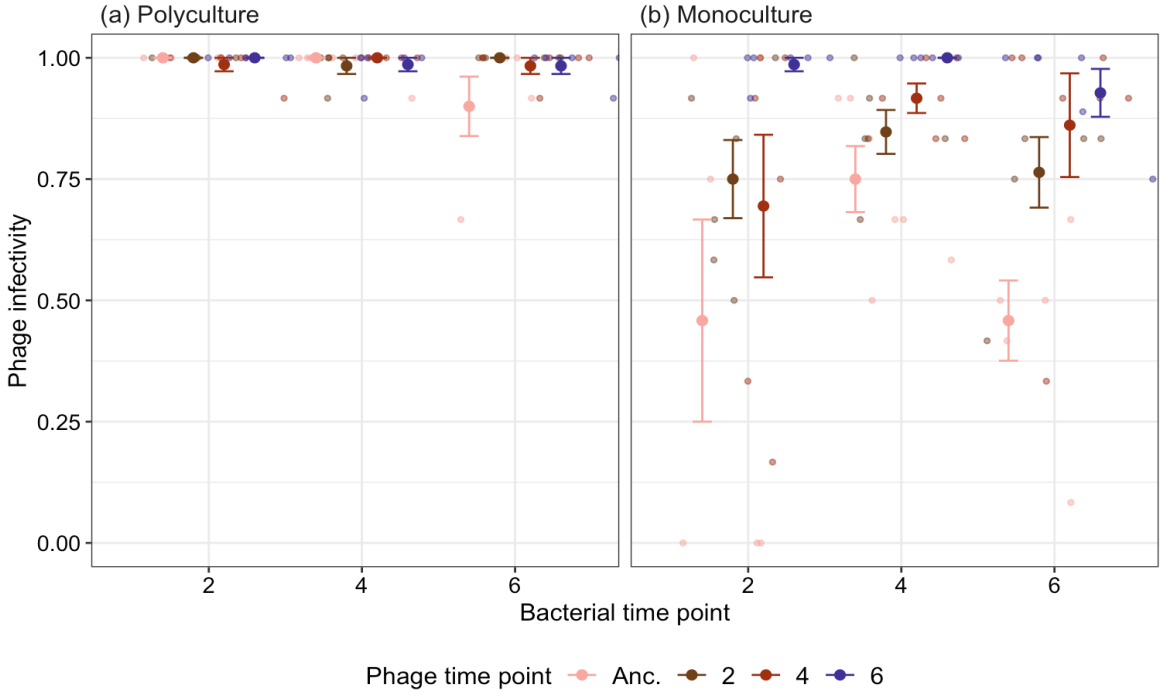

Figure S4. Changes in phage infectivity (the proportion of phage susceptible bacteria) to *Ochrobactrum* through time, demonstrated by assaying phages from different time-points against bacteria from different time-points. Points with bars represent the means with standard errors. Individual points represent separate treatment replicates.

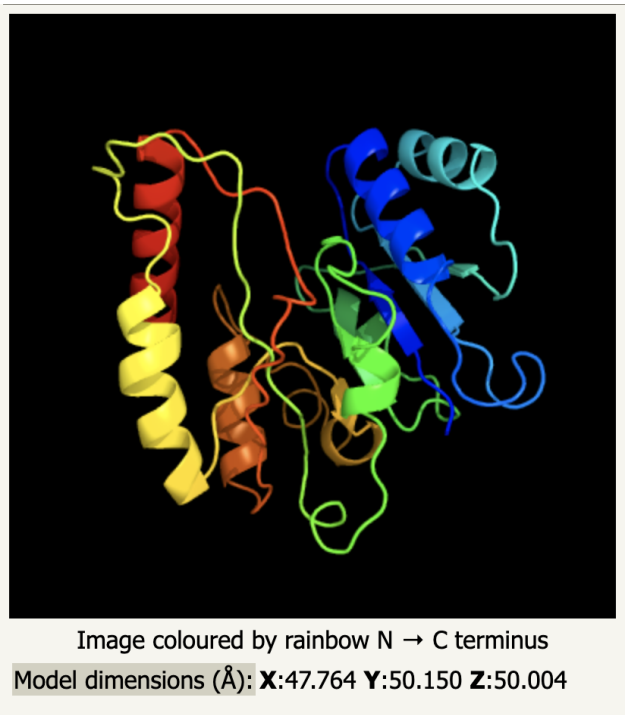

Figure S5. Predicted protein structure of an identified hypothetical protein, mutated in phage resistant isolates. This protein held 99% similarity to membrane protein cellulose synthase. Protein predicted and visualised using Phyre2 with 99.7% confidence.

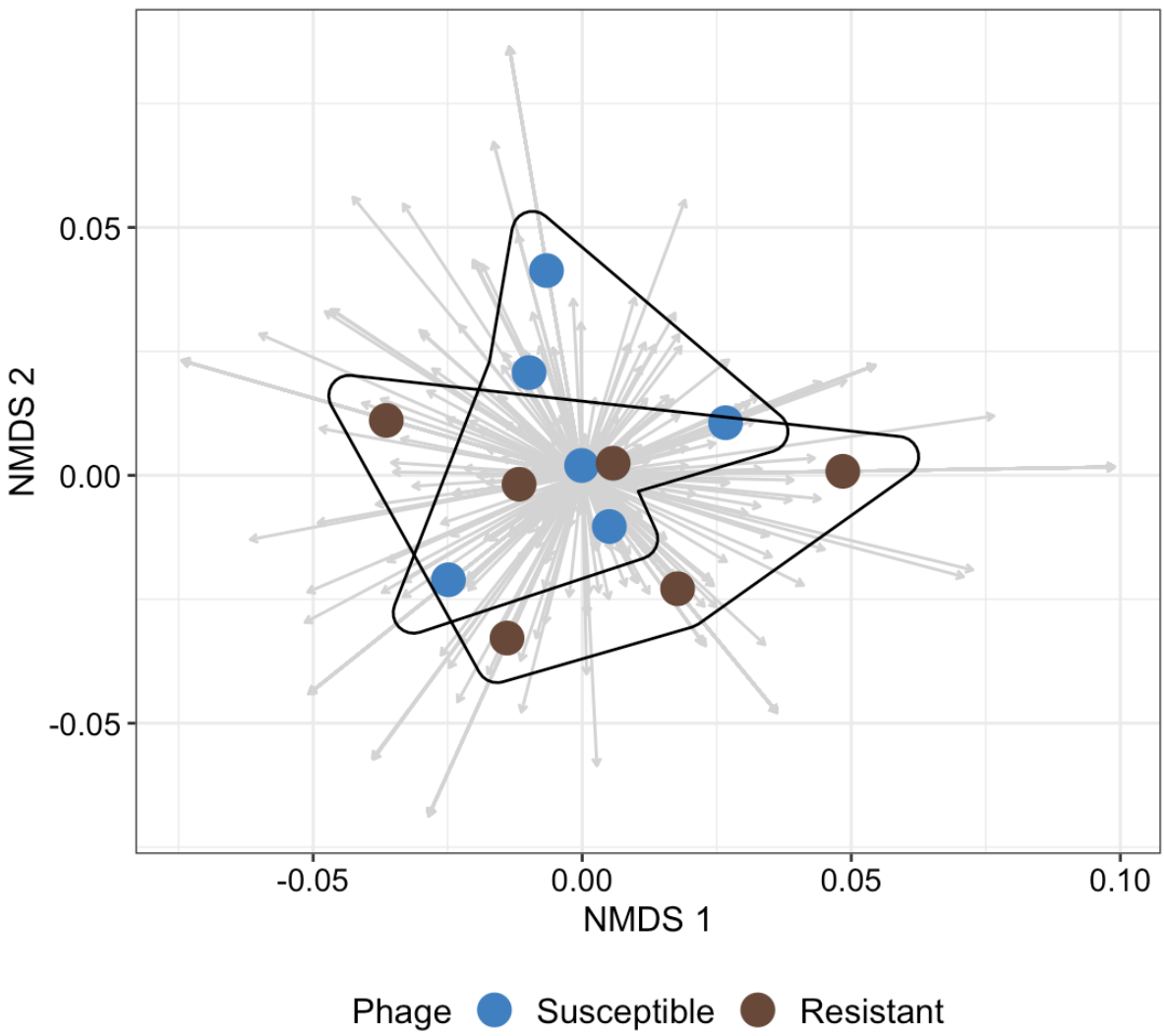

647

648 Figure S6. The divergence of each treatment group as indicated by Euclidean
649 distances of each gene (arrows) from the ancestral genome. Points represent
650 individual replicates sequenced from phage resistant or susceptible treatment groups.

651

652 Table S1. Tukey HSD contrasts comparing *Variovorax* densities in polyculture (poly.)
653 and monoculture (mono.) through time. P-values adjusted using the Tukey method of
654 comparing a family of three estimates.

Contrast	Week	Estimate	t-ratio	p-value
Poly. - Mono.	2	0.530	7.202	<0.001
Poly. - Mono.	4	0.406	5.519	<0.001
Poly. - Mono.	6	0.062	0.842	0.402
Poly. - Mono.	8	0.060	0.822	0.413

655
656
657
658 **References**

659 1. Chevallereau A, Pons BJ, van Houte S, Westra ER. Interactions between bacterial and
660 phage communities in natural environments. *Nat Rev Microbiol* 2022; **20**: 49–62.
661 2. Winter C, Bouvier T, Weinbauer MG, Thingstad TF. Trade-Offs between Competition
662 and Defense Specialists among Unicellular Planktonic Organisms: the 'Killing the
663 Winner' Hypothesis Revisited. *Microbiol Mol Biol Rev* 2010; **74**: 42–57.
664 3. Chan BK, Sistrom M, Wertz JE, Kortright KE, Narayan D, Turner PE. Phage selection
665 restores antibiotic sensitivity in MDR Pseudomonas aeruginosa. *Sci Rep* 2016; **6**: 26717.
666 4. Markwitz P, Lood C, Olszak T, van Noort V, Lavigne R, Drulis-Kawa Z. Genome-
667 driven elucidation of phage-host interplay and impact of phage resistance evolution on
668 bacterial fitness. *ISME J* 2021.
669 5. Breitbart M, Bonnain C, Malki K, Sawaya NA. Phage puppet masters of the marine
670 microbial realm. *Nat Microbiol* 2018; **3**: 754–766.
671 6. Jensen MA, Faruque SM, Mekalanos JJ, Levin BR. Modeling the role of bacteriophage
672 in the control of cholera outbreaks. *Proc Natl Acad Sci USA* 2006; **103**: 4652–4657.

673 7. Oechslin F. Resistance Development to Bacteriophages Occurring during Bacteriophage
674 Therapy. *Viruses* 2018; **10**: 351.
675 8. Abedon ST. Use of phage therapy to treat long-standing, persistent, or chronic bacterial
676 infections. *Adv Drug Deliv Rev* 2019; **145**: 18–39.
677 9. Hampton HG, Watson BNJ, Fineran PC. The arms race between bacteria and their
678 phage foes. *Nature* 2020; **577**: 327–336.
679 10. Mizoguchi K, Morita M, Fischer CR, Yoichi M, Tanji Y, Unno H. Coevolution of
680 Bacteriophage PP01 and *Escherichia coli* O157:H7 in Continuous Culture. *Appl*
681 *Environ Microbiol* 2003; **69**: 170–176.
682 11. Buckling A, Rainey PB. Antagonistic coevolution between a bacterium and a
683 bacteriophage. *Proc Royal Soc B* 2002; **269**: 931–936.
684 12. Dewald-Wang EA, Parr N, Tiley K, Lee A, Koskella B. Multiyear Time-Shift Study of
685 Bacteria and Phage Dynamics in the Phyllosphere. *The American Naturalist* 2022; **199**:
686 126–140.
687 13. Osada K, Takeuchi I, Miyanaga K, Tanji Y. Coevolution between Staphylococcus
688 aureus isolated from mastitic milk and its lytic bacteriophage ΦSA012 in batch co-
689 culture with serial transfer. *Biochemical Engineering Journal* 2017; **126**: 16–23.
690 14. Gandon S, Buckling A, Decaestecker E, Day T. Host-parasite coevolution and patterns
691 of adaptation across time and space. *J Evol Biol* 2008; **21**: 1861–1866.
692 15. Gómez P, Buckling A. Bacteria-Phage Antagonistic Coevolution in Soil. *Science* 2011;
693 **332**: 106–109.
694 16. Koskella B, Parr N. The evolution of bacterial resistance against bacteriophages in the
695 horse chestnut phyllosphere is general across both space and time. *Phil Trans R Soc B*
696 2015; **370**: 20140297.

697 17. LeGault KN, Hays SG, Angermeyer A, McKitterick AC, Johura F, Sultana M, et al.
698 Temporal shifts in antibiotic resistance elements govern phage-pathogen conflicts.
699 *Science* 2021; **373**: eabg2166.
700 18. Piel D, Bruto M, Labreuche Y, Blanquart F, Goudenège D, Barcia-Cruz R, et al. Phage–
701 host coevolution in natural populations. *Nat Microbiol* 2022; **7**: 1075–1086.
702 19. Castledine M, Padfield D, Buckling A. Experimental (co)evolution in a multi-species
703 microbial community results in local maladaptation. *Ecol Lett* 2020; **23**: 1673–1681.
704 20. Friman V-P, Buckling A. Effects of predation on real-time host-parasite coevolutionary
705 dynamics. *Ecol Lett* 2013; **16**: 39–46.
706 21. Lawrence D, Fiegna F, Behrends V, Bundy JG, Phillimore AB, Bell T, et al. Species
707 Interactions Alter Evolutionary Responses to a Novel Environment. *PLoS Biol* 2012;
708 **10**: e1001330.
709 22. Harrison E, Hall JPJ, Paterson S, Spiers AJ, Brockhurst MA. Conflicting selection alters
710 the trajectory of molecular evolution in a tripartite bacteria-plasmid-phage interaction.
711 *Mol Ecol* 2017; **26**: 2757–2764.
712 23. Hall JPJ, Harrison E, Brockhurst MA. Competitive species interactions constrain abiotic
713 adaptation in a bacterial soil community. *Evolution Letters* 2018; **2**: 580–589.
714 24. Scanlan PD, Hall AR, Blackshields G, Friman V-P, Davis MR, Goldberg JB, et al.
715 Coevolution with Bacteriophages Drives Genome-Wide Host Evolution and Constrains
716 the Acquisition of Abiotic-Beneficial Mutations. *Molecular Biology and Evolution*
717 2015; **32**: 1425–1435.
718 25. Brockhurst MA, Morgan AD, Rainey PB, Buckling A. Population mixing accelerates
719 coevolution. *Ecology Letters* 2003; **6**: 975–979.

720 26. Castledine M, Newbury A, Lewis R, Hacker C, Meaden S, Buckling A. Antagonistic
721 Mobile Genetic Elements Can Counteract Each Other's Effects on Microbial
722 Community Composition. *mBio* 2023; e00460-23.
723 27. Brockhurst MA, Rainey PB, Buckling A. The effect of spatial heterogeneity and
724 parasites on the evolution of host diversity. *Proc R Soc Lond B* 2004; **271**: 107–111.
725 28. Padfield D, Castledine M, Pennycook J, Hesse E, Buckling A. Short-term relative
726 invader growth rate predicts long-term equilibrium proportion in a stable, coexisting
727 microbial community. *bioRxiv* 2020.
728 29. Morgan AD, Gandon S, Buckling A. The effect of migration on local adaptation in a
729 coevolving host–parasite system. *Nature* 2005; **437**: 253–256.
730 30. Deatherage DE, Barrick JE. Identification of mutations in laboratory-evolved microbes
731 from next-generation sequencing data using breseq. *Methods Mol Biol* 2014; **1151**: 165–
732 188.
733 31. Kelley LA, Mezulis S, Yates CM, Wass MN, Sternberg MJE. The Phyre2 web portal for
734 protein modeling, prediction and analysis. *Nat Protoc* 2015; **10**: 845–858.
735 32. Walker-Sünderhauf D, Klümper U, Gaze WH, Westra ER, van Houte S. Interspecific
736 competition can drive the loss of conjugative plasmids from a focal species in a
737 microbial community. *bioRxiv* 2022.
738 33. Lenski RE, Rose MR, Simpson SC, Tadler SC. Long-Term Experimental Evolution in
739 Escherichia coli. I. Adaptation and Divergence During 2,000 Generations. *Am Nat* 1991;
740 **138**: 1315–1341.
741 34. Team RC. R: a language and environment for statistical computing. 2013.
742 35. Wickham H. ggplot2: elegant graphics for data analysis. 2016. Springer, New York.
743 36. Lenth R. Emmeans: Estimated marginal means, aka least-squares means. 2018. R
744 Package Version.

745 37. Oksanen J, Simpson GL, Blanchet FG, Kindt R, Legendre P, Minchin PR, et al. vegan:
746 Community Ecology Package. 2019.
747 38. Satola B, Wübbeler JH, Steinbüchel A. Metabolic characteristics of the species
748 Variovorax paradoxus. *Appl Microbiol Biotechnol* 2013; **97**: 541–560.
749 39. Griffin AS, West SA, Buckling A. Cooperation and competition in pathogenic bacteria.
750 *Nature* 2004; **430**: 1024–1027.
751 40. Salathé M, Soyer OS. Parasites lead to evolution of robustness against gene loss in host
752 signaling networks. *Mol Syst Biol* 2008; **4**: 202.
753 41. Lythgoe KA, Chao L. Mechanisms of coexistence of a bacteria and a bacteriophage in a
754 spatially homogeneous environment. *Ecol Letters* 2003; **6**: 326–334.
755 42. Giovannoni SJ. SAR11 Bacteria: The Most Abundant Plankton in the Oceans. *Annu Rev*
756 *Mar Sci* 2017; **9**: 231–255.
757 43. Castledine M, Padfield D, Sierocinski P, Soria Pascual J, Hughes A, Mäkinen L, et al.
758 Parallel evolution of Pseudomonas aeruginosa phage resistance and virulence loss in
759 response to phage treatment in vivo and in vitro. *eLife* 2022; **11**: e73679.
760